Russian Journal of General Chemistry, Vol. 72, No. 5, 2002, pp. 748–759. Translated from Zhurnal Obshchei Khimii, Vol. 72, No. 5, 2002, pp. 802–813.

Quantum-Chemical Study of the Mechanism of Hydrocarbon Oxidation with Molecular Oxygen

E. V. Nikolaeva, A. G. Shamov, G. M. Khrapkovskii, and Kh. E. Kharlampidi

Kazan State University of Technology, Kazan, Tatarstan, Russia

Received April 7, 2000

Abstract—The minimal kinetic scheme of the mechanism of hydrocarbon oxidation with molecular oxygen was studied by the PM3 semiempirical quantum-chemical method and also by the B3LYP hybrid density functional method using the 3-21G and 6-21G(d) basis sets and the GAUSSIAN 94 software. The energy characteristics and structural parameters of the reactants, products, and transition states of some elementary stages were determined. The simplest hydrocarbons, methane and ethane, were taken as substrates. For same reactions the effect of substituents, including bulky groups (methylbenzene, ethylbenzene, isopropylbenzene), was considered.

Oxidation of hydrocarbons with molecular oxygen is the key stage in novel processes for production of many important chemicals. Therefore, it is extremely important to find the best oxidation conditions to attain the highest yield of the target products and reduce the production cost. To find such optimal conditions, it is necessary to gain insight into the reaction mechanism [1].

The chain mechanism of hydrocarbon oxidation was studied in detail experimentally [2–6]. Various alternatives were suggested [7–11], and the kinetic parameters were determined for some elementary stages of the process [12–15]. However, many questions are still unanswered because of problems with identification of radicals and lack of reliable energy data for particular stages of the reaction mechanism. At the same time, it is quite obvious that specifically the energy characteristics primarily determine the probability of occurrence of chemical processes.

Recent rapid progress of the quantum chemistry and computation facilities made it possible in certain cases to evaluate the barriers of elementary stages of multistage chemical reactions with experimental accuracy. Therefore, quantum-chemical studies will aid in overcoming difficulties arising in experimental study of the oxidation mechanism.

Separate stages of hydrocarbon oxidation were examined theoretically in numerous papers [9, 16, 17]. However, published data are fragmentary and do not allow the process to be considered as a whole from a unified standpoint.

In this work we took advantage of quantum-chemical methods to study the mechanism of hydrocarbon oxidation. Our study involved construction of the most interesting regions of the polydimensional potential energy surface and search for extrema corresponding to transition states of chemical reactions. From the revealed transition states, we descended along the reaction path to reactants and products of an elementary stage of a chemical transformation. By this procedure, we evaluated the activation energies of the direct and reverse reactions. In all cases the transition states were proved by the presence of a single negative value in the matrix of second derivatives. The correspondence of the transition states to the processes under consideration was checked by descending to reactants and products along the internal reaction coordinates.

All the results given below were obtained using the GAUSSIAN 94 software [18]. The potential energy surfaces were constructed by the PM3 semiempirical method [19] and by the B3LYP density functional method [18, 20, 21] with allowance for electron correlation.

Study of the oxidation mechanism as a whole is a very complex problem, and in this work we have restricted ourselves to determining the energy characteristics of certain key stages in the minimal kinetic scheme of the process accepted by the majority of researchers [1, 3, 5, 7, 9]. An important prerequisite for successful use of quantum-chemical methods for studying the oxidation mechanism is availability of reliable experimental data on the process kinetics and composition of products in various stages. Our anal-

1070-3632/02/7205-0748 $27.00

ysis of published experimental data shows that for many elementary stages the activation energies vary in a wide range, and for some stages such data are lacking at all (Table 1). In Table 1 we also present the activation energies obtained by us using various quantum-chemical methods [22, 23].

Table 1. Barriers of some elementary stages of hydrocarbon oxidation[a]

Elementary stage	This work		Published data		
	calculation method	E_a, kJ mol^{-1}	E_a(exp.), kJ mol^{-1}	experimental conditions, calculation method	references
RH + O_2 ⟶ R$^\cdot$ + $HO_2^\cdot$ (R = CH_3) (0)	PM3	199.03 (35.95)	221.65± 19.27	1535–185 K, shock waves	[24]
			226.26	Study of initiation kinetics	[6]
R$^\cdot$ + O_2 ⟶ $RO_2^\cdot$ (R = CH_3) (1)	PM3	38.63 (109.23)	8.38	Gas phase, 285–460°C, 280–420 mm Hg	[8]
			0	Gas phase, 473 K, photolysis of $(CH_3)_2CO$	[24]
			~1.68	Gas phase, 396 K	[24]
$RO_2^\cdot$ + RH ⟶ ROOH + R$^\cdot$ (2)					
RH + HOO$^\cdot$ ⟶ R$^\cdot$ + HOOH (R = CH_3) (3)	PM3 (RHF)	130.8	–	–	–
(R = Ph–CH_2)	PM3 (RHF)	125.70	–	–	–
(R = Ph–C(H)CH_3)	PM3 (RHF)	117.53	–	–	–
(R = Ph–C$(CH_3)_2$)	PM3 (RHF)	111.12	–	–	–
$RO_2^\cdot$ + RH ⟶ ROOH + R$^\cdot$ (R = CH_3) (4)	PM3	98.38	~50.6	Parabolic model	[13]
	PM3	126.16	~77.44	E_a –113 + 0.45$Q_{C–H}$	[1]
	(RHF)		38.13	–	[6]
	B3LYP/ 6-31G(d) (RHF)	111.58	~113.13	Measurement of the ratio $k_2k_6^{-1/2}$ (k_2 – $RO_2^\cdot$ + RH, k_6 – $RO_2^\cdot$ + $RO_2^\cdot$)	[4]
(R = Ph–CH_2)	PM3 (RHF)	121.68	~51.04	E_a –113 + 0.45$Q_{C–H}$	[1]
(R = Ph–C(H)CH_3)	PM3	117.78	35.62	Liquid phase	[4,6]
	(RHF)		~41.61	E_a –113 + 0.45$Q_{C–H}$	[1]
(R = Ph–C$(CH_3)_2$)	PM3	97.88	28.07	Liquid phase	[4,6]
	(RHF)		~39.73	E_a –113 + 0.45$Q_{C–H}$	[1]
ROOH ⟶ RO$^\cdot$ + HO$^\cdot$ (R = CH_3) (5)	PM3	114.64 (9.93)	181±18.8	Calculation	[25]
	B3LYP/ 3-21G	179.84 (14.54)	134	Pyrolysis in a mixture with toluene vapor by jet procedure, gas phase, 565–651 K, low pressure	[14]
	B3LYP/ 6-31G(d)	170.98 (8.97)			
(R = C_2H_5)	PM3	112.21 (10.68)	158	Pyrolysis in a mixture with toluene by jet procedure, gas phase, 553–653 K, low pressure	[14]
	B3LYP/ 6–31G(d)	147.99 (6.79)	159.22	Gas phase	[6]
			211.29±8.3 (0)	Calculation	[25]
				From the rate constant of reverse reaction and equilibrium constant, gas phase, 565–655 K	[24]
ROOH + R'O$^\cdot$ ⟶ R'OH + ROO$^\cdot$ (6)					
(R = CH_3, R' = H) (7)	PM3	84.47 (124.07)	–	–	–

Table 1. (Contd.)

Elementary stage	This work		Published data		
	calculation method	E_a, kJ mol^{-1}	E_a(exp.), kJ mol^{-1}	experimental conditions, calculation method	references
(R = R' = CH_3) (8)	PM3	110.11 (111.71)	–	–	–
2 ROOH ⟶ $RO_2^{\cdot}$ + $RO^{\cdot}$ + H_2O (9)	PM3	160.18	–	–	–
(R = CH_3)		(108.94)			
	B3LYP/ 3-21G	113.66 (63.81)	–	–	–
(R = CH_3)	B3LYP/ 6-31G(d)	91.15 (49.29)	–	–	–
$RO^{\cdot}$ ⟶ R'=O + $CH_3^{\cdot}$ (10)	PM3	96.39	83.8	Gas phase, 285–460°C, 280–420 mm	[8]
(R = C_2H_5, R' = CH_2)		(52.32)			
	B3LYP/ 6-31G(d)	83.51	54.47	Photolysis of $C_2H_5COOC_2H_5$, 302–468 K	[24]
	(RHF)		~96.37	Estimation, 318–418 K	[24]
(R = Ph–C(H)CH_3)	PM3	77.75 (61.86)	–	–	–
(R = Ph–C(CH_3)$_2$)	PM3	60.02 (72.67)	–	–	–
$RO^{\cdot}$ ⟶ R'=O + $H^{\cdot}$ (R = Ph–CH_2)	PM3	69.46 (0.03)	–	–	–
(R = Ph–C(H)CH_3)	PM3	59.37 (1.10)	–	–	–
$ROO^{\cdot}$ ⟶ R'=O + R''$O^{\cdot}$ (11)					
(R = CH_3):					
$CH_3OO^{\cdot}$ ⟶ CH_2O–$^{\cdot}$OH (12)	PM3	161.9 (297.6)	83.8	Gas phase, 285–460°C, 280–420 mm Hg	[8]
CH_2O–$^{\cdot}$OH ⟶ CH_2=O + $HO^{\cdot}$ (13)	PM3	18.31 (4.37)			
(R = C_2H_5):					
$C_2H_5O_2^{\cdot}$ ⟶ C_2H_4O–$^{\cdot}$OH	PM3	152.35 (305.53)	121.51	Mathematical simulation based on experimental data	[9]
			211	*Ab initio* quantum-chemical calculation	[16]
C_2H_4O–$^{\cdot}$OH ⟶ C_2H_4O + $HO^{\cdot}$	PM3	13.41 (16.47)	–	–	–
$C_2H_5O_2^{\cdot}$ ⟶ CH_2O–$^{\cdot}$$OCH_3$ (14)	PM3	260.74 (431.49)	121.51	Mathematical simulation based on experimental data	[9]
CH_2O–$^{\cdot}$$OCH_3$ ⟶ CH_2O + $CH_3O^{\cdot}$ (14')	PM3	2.6 (19.15)	–	–	–
ROOH ⟶ R'=O + R''OH (15)					
(R = CH_3):					
CH_3OOH ⟶ CH_2O–OH_2 (16)	PM3	128.88 (339.10)	–	–	–

Table 1. (Contd.)

Elementary stage	This work		Published data		
	calculation method	E_a, kJ mol^{-1}	E_a(exp.), kJ mol^{-1}	experimental conditions, calculation method	references
$CH_3O–OH_2 \longrightarrow CH_2O + H_2O$ (17)	PM3	0.2 (18.48)	–	–	–
(R = C_2H_5):					
$C_2H_5OOH \longrightarrow C_2H_4O–OH_2$	PM3	129.85 (344.29)	–	–	–
$C_2H_4O–OH_2 \longrightarrow C_2H_4O + H_2O$	PM3	~0 (20.32)	–	–	–
$C_2H_5OOH \longrightarrow CH_2O + CH_3OH$ (18)	PM3	259.99 (447.91)	–	–	–
$RO^{\cdot} + CH_2O \longrightarrow ROH + H–C^{\cdot}=O$ (19)			2.095	Electric discharge, gas phase	[24]
(R = H) (20)	PM3	25.00 (157.52)		346–489 K	
			~8.38	Thermal pathway, gas phase, 588 K	[24]
			17.6	*Ab initio* quantum-chemical calculation	[16]
			54.47	Flame, gas phase, 1250–1550 K	[22]
(R = CH_3) (21)	PM3	44.83 (116.46)	12.57	Photolysis, 455 K, gas phase	[24]
$H–C^{\cdot}=O + H_2O \longrightarrow HCOOH + H^{\cdot}$ (22)	PM3	131.23 (35.15)	–	–	–
$H–C^{\cdot}=O \longrightarrow CO + H^{\cdot}$ (23)	PM3	153.98 (1.75)	54.47	Photolysis of HCHO, 430–568 K, gas phase	[24]
			79.61	Mathematical simulation based on experimental data	[9]
			113.13	Pressure of fuel–oxygen mixture <1 atm, 100–500°C, gas phase	[5]
$HCOOH \longrightarrow H_2 + CO_2$ (24)	PM3	356.49 (390.72)	–	–	–

[a] The barriers of the reverse reactions are given in parentheses.

Comparison of the left and right parts of Table 1 shows that our results allow the mechanism of hydrocarbon oxidation with molecular oxygen to be considered from a unified standpoint.

Let us discuss in more detail the results that we think to be the most interesting. For convenience sake, we will follow a classical scheme distinguishing the elementary stages of chain initiation, propagation, degenerate branching, and termination and consider data for each of these groups of reactions.

As a chain initiation stage we considered the bimolecular reaction of a hydrocarbon with oxygen

$$RH + O_2 \longrightarrow R^{\cdot} + HO_2^{\cdot},$$

namely,

$$CH_4 + O_2 \longrightarrow CH_3^{\cdot} + HOO^{\cdot} \quad (0)$$

This process is the limiting stage of the whole oxidation process, and we used its estimated activation energy, which is very close to the experimental value (Table 1), as a comparative criterion when assessing the feasibility of one or another elementary stage.

The main geometries of the reactants, transition state, and products of reaction (0) are given in Table 2.

Table 2. Geometries of the reactants, products, and transition state of reaction (0)[a]

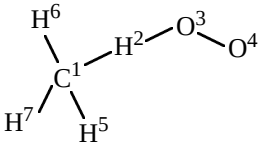

Parameter	CH_4 + O=O	Transition state	$CH_3^{\cdot}$ + $HO_2^{\cdot}$
C^1–H^2	109.4	138.6	232
H^2–O^3	194.0	110.96	96.0
O^3–O^4	116.9	121.6	126.5
C^1–H^5	108.6	107.9	107.3
C^1–H^6	108.7	107.9	107.3
C^1–H^7	108.7	107.9	107.3
$\angle C^1H^2O^3$	179.29	175.39	178.51
$\angle H^2O^3O^4$	128.85	111.08	107.53
$\angle H^5C^1H^2$	109.46	103.35	90.75
$\angle H^6C^1H^2$	109.45	104.05	93.21
$\angle H^7C^1H^2$	109.40	104.05	93.31
$\angle C^1H^2O^3O^4$	1.81	–179.89	–1.02
$\angle H^5C^1H^2O^3$	–2.21	179.85	1.08
$\angle H^6C^1H^2O^3$	117.80	–60.23	–118.86
$\angle H^7C^1H^2O^3$	–122.23	59.93	121.01

[a] Here and in Tables 3 and 5–13, the bond lengths are given in pm, and the angles, in degrees.

Table 3. Geometries of the reactants, products, and transition state of reaction (1)

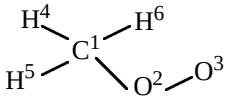

Parameter	$CH_3^{\cdot}$ + O=O	Transition state	$CH_3OO^{\cdot}$
C^1–O^2	362.7	202.5	143.8
O^2–O^3	116.9	117.9	126.2
C^1–H^4	107.2	107.8	109.4
C^1–H^5	107.3	107.8	109.3
C^1–H^6	107.3	107.8	109.6
$\angle C^1O^2O^3$	98.71	116.93	114.89
$\angle H^4C^1O^2$	98.66	99.09	105.70
$\angle H^5C^1H^4$	120.04	116.70	110.07
$\angle H^6C^1H^4$	120.03	116.67	110.13
$\angle H^4C^1O^2O^3$	–0.05	–120.52	–122.39
$\angle H^5C^1O^2O^3$	–119.828	120.39	120.85
$\angle H^6C^1H^4H^5$	179.71	144.54	121.57

Table 4. Geometries of the transition state of reaction (3)

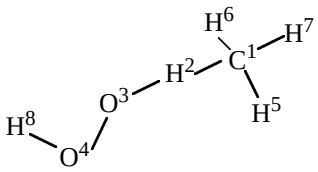

Bond length		Bond angle		Torsion angle	
bond	*d*, pm	angle	ω, deg	angle	τ, deg
C^1–H^2	124.3	$C^1H^2O^3$	174.02	$C^1H^2O^3O^4$	–167.77
H^2–O^3	123.2	$H^2O^3O^4$	107.00	$H^2O^3O^4H^8$	91.56
O^3–O^4	138.0	$O^3O^4H^8$	111.34	$H^5C^1H^2O^3$	119.76
O^4–H^8	94.1	$H^5C^1H^2$	119.76	$H^6C^1H^2O^3$	–0.31
H^5–C^1	108.1	$H^6C^1H^2$	105.83	$H^7C^1H^2O^3$	–120.34
H^6–C^1	108.1	$H^7C^1H^2$	105.41		
H^7–C^1	108.1				

A specific feature of the initiation reaction is formation of a prereaction hydrogen-bonded complex (H^2–O^3 bond in reactants, Table 2), which decreases somewhat the overall energy of the reactants as compared to the sum of the energies of the initial molecules separated by an infinite distance.

We considered two chain propagation reactions (Table 3): reaction of the alkyl radical with oxygen (1) and formation of alkyl hydroperoxide (2):

$$R^{\cdot} + O_2 \longrightarrow RO_2^{\cdot}, \quad (1)$$

$$RO_2^{\cdot} + RH \longrightarrow ROOH + R^{\cdot}, \quad (2)$$

$$R = CH_3.$$

The energy barrier of reaction (1), according to our calculations, exceeds the experimental estimate (Table 1).

For elementary stage (2), we considered two cases: reaction of hydrocarbons with hydroperoxyl (Table 4) and alkylperoxyl radicals:

$$HOO^{\cdot} + RH \longrightarrow HOOH + R^{\cdot}, \quad (3)$$

$$ROO^{\cdot} + RH \longrightarrow ROOH + R^{\cdot}, \quad (4)$$

$$R = CH_3^{\cdot}$$

The activation energies of these two processes are close (130.8 and 126.16 kJ mol^{-1}, respectively), so that the reactions of $HO_2^{\cdot}$ and $RO_2^{\cdot}$ radicals with hydrocarbons can be competing (Table 1).

Table 5. Main geometries of the reactants, products, and transition state of reactions (5)

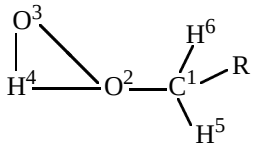

R	Method	Structure	C^1–O^2	O^2–O^3	O^3–H^4	O^2–H^4	$\angle C^1O^2O^3$	$\angle O^2O^3H^4$	$\angle C^1O^2O^3H^4$
H	PM3	Reactants	138.8	152.5	94.2	185.8	107.09	94.75	174.62
		Transition state	132.5	231.3	94.3	180.9	118.89	133.77	137.17
		Products	132.4	276.2	94.7	181.96	114.92	4.68	2.04
	B3LYP/	Reactants	146.1	152.4	100.3	192.6	102.5	97.2	140.2
	3-21G	Transition state	143.9	237.1	101.6	184.4	97.0	47.5	120.0
		Products	144.5	275.7	102.7	181.3	83.5	18.6	172.4
	B3LYP/	Reactants	141.7	145.6	97.4	188.4	106.1	99.8	115.3
	6-31G(d)	Transition state	137.4	250.8	98.2	203.9	50.1	51.1	116.6
		Products	137.5	286.7	99.0	193.8	92.2	16.5	172.3
CH_3	PM3	Reactants	139.7	152.7	94.2	185.6	107.93	94.48	175.64
		Transition state	132.99	238.4	93.8	251.0	116.14	86.66	–95.46
		Products	132.95	319.0	93.9	258.1	104.96	42.72	158.10
	B3LYP/	Reactants	142.7	145.9	97.4	188.7	106.74	99.83	116.74
	6-31G(d)	Transition state	137.6	255.4	98.3	201.69	105.62	47.03	123.98
		Products	137.5	290.3	98.99	194.1	105.75	11.06	158.10

Reactions (3) and (4) were studied for a series of hydrocarbons: methane, methylbenzene, ethylbenzene, and isopropylbenzene. In this order, the activation energy decreases, and hence the reactivity increases (Table 1).

With all the substituents under consideration, the reaction center has a similar structure. In the series methane, methylbenzene, ethylbenzene, isopropylbenzene the bond lengths in the reaction center of (4) increase (124.3, 125.5, 127.7, and 131.7 pm for the α-C–H bond and 123.2, 124.6, 128.3, and 131.0 pm for the H–O bond, respectively), which confirms the increase in the reactivity in this order.

The structures obtained for the transition states with small molecules (such as methane) can be good models for studying reactions of variously substituted compounds, because the main geometries of the reaction center are influenced by substituents insignificantly.

We would like to note the following, most interesting from our viewpoint, results obtained in studying elementary stages of degenerate chain branching.

For the reaction reverse to homolytic cleavage of hydrocarbon hydroperoxides (5), i.e., for recombination, our PM3 calculations revealed a small barrier, in contrast to commonly accepted views. The existence of the barrier was confirmed by *ab initio* calculations (Table 1).

$$ROOH \longrightarrow RO^{\cdot} + HO^{\cdot}. \quad (5)$$

As seen from Table 5, the H^4–O^2 bond length in the product is about 180–200 pm, which corresponds to the length of a hydrogen bond, evaluated by various procedures. Our results suggest that the possibility of formation of hydrogen-bonded complexes is largely responsible for appearance of a barrier to radical recombination.

Owing to the existence of a barrier, it becomes possible to reliably determine the structures of the transition states in radical reactions, including not only recombination but also reverse homolytic cleavage processes.

For elementary stage (6) we considered two alternatives (Table 6):

$$ROOH + RO^{\cdot} \longrightarrow ROO^{\cdot} + ROH, \quad (6)$$

$$RO^{\cdot} = HO^{\cdot}: CH_3OOH + HO^{\cdot} \longrightarrow CH_3OO^{\cdot} + H_2O, \quad (7)$$

$$RO^{\cdot} = CH_3O^{\cdot}: CH_3OOH + CH_3O^{\cdot} \longrightarrow CH_3OO^{\cdot} + CH_3OH. \quad (8)$$

Table 6. Main geometries of the reactants, products, and transition state of reactions (7) and (8)

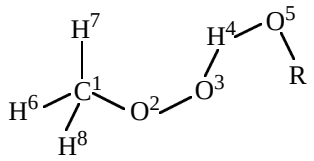

Parameter	$CH_3OOH + RO^{\cdot}$		Transition state		$CH_3OO^{\cdot} + ROH$	
	R = H	R = CH_3	R = H	R = CH_3	R = H	R = CH_3
O^3–H^4	94.7	94.6	103.3	111.0	183.7	181.6
H^4–O^5	180.7	182.2	114.0	105.5	94.5	95.4
$\angle O^2O^3H^4$	95.03	94.97	97.53	103.28	121.57	123.61
$\angle O^3H^4O^5$	82.69	86.26	131.70	105.50	89.36	91.02
$\angle H^4O^5R$	128.40	135.95	113.58	113.21	108.76	107.87
$\angle O^2O^3H^4O^5$	114.15	124.29	120.76	121.56	–99.50	96.40
$\angle O^3H^4O^5R$	–39.42	47.96	–39.80	90.66	–45.14	124.86

Comparison of the barriers of elementary stages (7) and (8) (Table 1) shows that the activation energy of (7) is lower by 25.64 kJ mol^{-1}. Hence, the reaction with the hydroxyl radical will be preferable to the reaction with the methoxy radical.

When studying a bimolecular reaction between hydrocarbon hydroperoxide molecules, we obtained an unexpected result: According to calculations, the reverse reaction is trimolecular:

$$2ROOH \longrightarrow RO_2^{\cdot} + RO^{\cdot} + H_2O, \quad (9)$$

$$R = CH_3.$$

It is known that trimolecular reactions are relatively seldom, and their occurrence should be specially proved in each particular case. Such a proof is offered by quantum-chemical calculations.

PM3 calculations show that, although the estimated energy barrier of reaction (9) does not exceed the barrier of the limiting stage, occurrence of this reaction in two stages [homolytic cleavage (5) and reaction of the hydroxy radical with the second hydroperoxide molecule (7)] is more probable.

However, B3LYP calculations with the 3-21G and 6-31G(d) basis sets refuted this assumption (Table 1) and gave the results consistent with the experiment [4, 6]. Formation of a hydrogen bond between two alkyl hydroperoxide molecules (Table 7) somewhat decreases the energy of formation of the reactant complex relative to the sum of the energies of alkyl hydroperoxide molecules separate by an infinite distance; the barrier of reaction (9) thereby increases by 16–25 kJ mol^{-1}, according to different estimates. However, formation of this bond decreases the barrier of the bimolecular reaction of alkyl hydroperoxides (113.79 and 91.15 kJ mol^{-1}) compared to the homolytic cleavage of the O–O bond (179.79 and 170.98 kJ mol^{-1}).

Disproportionation of alkoxyl radicals (10) was studied for a number of species derived from ethane (R = C_2H_5, R' = CH_2, R'' = CH_3), methylbenzene (R = $PhCH_2$, R' = PhCH, R'' = H), ethylbenzene [R = $PhC(H)CH_3$, R' = PhCH, R'' = CH_3 and R = $PhC(H)\cdot CH_3$, R' = $PhC(CH_3)$, R'' = H], and isopropylbenzene [R = $PhC(CH_3)_2$, R' = $PhC(CH_3)$, R'' = CH_3]:

$$RO^{\cdot} \longrightarrow R'O + R''^{\cdot}. \quad (10)$$

The activation energy of reaction (10) decreases in going from the ethyl to isopropyl (R'' = CH_3) substituent, whereas the barrier of reverse reactions increases. That is, the isopropoxyl radical is more reactive than the ethoxyl radical.

With the oxyl radical derived from ethylbenzene, two alternative reactions are possible: formation of acetophenone (R'' = H) and benzaldehyde (R'' = CH_3), as the activation barriers of these reactions differ insignificantly (by 18.38 kJ mol^{-1}) (Table 1).

Because the bond pattern in the reaction center of the transition state does not noticeably change in going from one substituents to another (Table 8), the activation energy of this reaction should not depend significantly on steric factors.

Table 7. Main geometries of the reactants, products, and transition state of reaction (9)

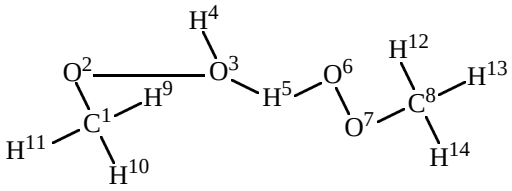

Parameter	$2CH_3OOH$, PM3	Transition state			$CH_3O^{\cdot} + CH_3OO^{\cdot} + H_2O$, PM3
		PM3	B3LYP/3-21G	B3LYP/6-31G(d)	
$C^1–O^2$	138.6	133.88	143.97	138.7	133.7
$O^2–O^3$	154.6	188.7	191.9	188.7	195.2
$O^3–H^5$	181.0	104.3	109.2	115.8	95.7
$H^5–O^6$	94.9	116.3	113.1	121.7	183.3
$O^6–O^7$	152.7	139.1	145.1	138.5	128.2
$O^7–C^8$	139.2	140.8	148.0	142.7	143.0
$\angle C^1O^2O^3$	107.62	110.59	100.31	102.6	111.59
$\angle O^2O^3H^5$	139.38	104.3	135.13	137.7	103.59
$\angle O^3H^5O^6$	90.21	127.86	145.68	153.5	85.71
$\angle H^5O^6O^7$	94.05	103.1	101.48	104.0	122.39
$\angle O^6O^7C^8$	105.08	111.1	104.48	108.2	114.06
$\angle C^1O^2O^3H^5$	94.51	–130.97	96.65	88.6	108.09
$\angle O^2O^3H^5O^6$	–145.43	–167.18	170.41	176.8	–156.52
$\angle O^3H^5O^6O^7$	108.19	108.9	80.88	90.8	83.39
$\angle H^5O^6O^7C^8$	–174.97	–111.17	–85.68	–110.1	–120.18

Table 8. Effect of substituents on the geometry of the reaction center of reaction (10). Transition state:

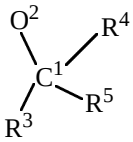

Method	Bond	Radicals R^5, R^3, and R^4, respectively				
		H, H, CH_3	Ph, H, CH_3	Ph, CH_3, CH_3	Ph, H, H	Ph, CH_3, H
PM3 (RHF)	$C^1–R^4$	194.1	193.7	193.5	156.2	159.7
	$C^1–O^2$	124.1	125.0	126.2	123.2	122.9
PM3 (UHF)	$C^1–R^4$	195.1	195.2	195.3	160.5	156.2
	$C^1–O^2$	124.7	125.8	127.0	122.5	124.1

We have also studied disproportionation of the peroxyl radical:

$$RO_2^{\cdot} \longrightarrow R'O + R''O^{\cdot}. \qquad (11)$$

The first stage involves isomerization, and this is the limiting stage of the overall process (11). This is followed by fast, almost barrier-free, dissociation of the resulting isomer (Table 1):

$$ROO^{\cdot} \longrightarrow R'O–{}^{\cdot}OR'', \qquad (12)$$

$$R'O–{}^{\cdot}OR'' \longrightarrow R'O + R''O^{\cdot}. \qquad (13)$$

Table 9. Main geometries of the reactants, products, and transition states of reactions (12) and (13). Transition states:

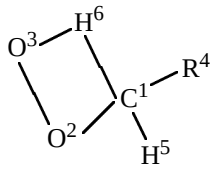

(12)

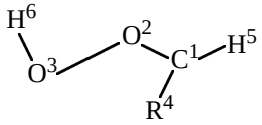

(13)

Parameter	Reactants				Transition state			
	reaction (12)		reaction (13)		reaction (12)		reaction (13)	
	R^4 = H	R^4 = CH_3	R^4 = H	R^4 = CH_3	R^4 = H	R^4 = CH_3	R^4 = H	R^4 = CH_3
C^1–O^2	143.8	145.1	120.8	121.4	134.5	136.3	120.4	121.1
O^2–O^3	126.2	126.2	193.1	193.4	160.1	157.4	233.3	232.5
C^1–H^6	109.5	110.6	329.2	333.7	137.2	138.1	344.9	347.7
O^3–H^6	243.3	253.8	93.8	93.8	139.3	141.0	93.7	93.7
$\angle C^1O^2O^3$	114.89	115.08	113.42	121.52	87.83	89.24	115.4	122.98
$\angle O^2O^3H^6$	61.58	65.0	101.75	97.88	82.61	82.79	86.68	83.68
$\angle H^6C^1O^2$	111.9	111.15	28.9	22.43	93.7	92.21	28.8	22.97
$\angle C^1O^2O^3H^6$	1.15	44.96	166.84	–178.56	0.0	2.24	–174.09	–179.15
$\angle O^2O^3H^6C^1$	1.15	44.96	–6.72	0.61	0.0	2.24	2.21	1.89

Parameter	Products			
	reaction (12)		reaction (13)	
	R^4 = H	R^4 = CH_3	R^4 = H	R^4 = CH_3
C^1–O^2	120.8	121.5	120.3	121.1
O^2–O^3	193.1	193.4	328.7	322.9
C^1–H^6	329.2	333.5	364.9	326.2
O^3–H^6	93.8	93.8	95.4	93.9
$\angle C^1O^2O^3$	113.42	121.25	114.67	112.05
$\angle O^2O^3H^6$	101.75	97.88	28.19	28.55
$\angle H^6C^1O^2$	28.9	22.60	17.2	39.16
$\angle C^1O^2O^3H^6$	166.84	–178.43	–179.16	–178.82
$\angle O^2O^3H^6C^1$	–6.72	0.63	0.33	0.31

Here for methylperoxyl radical R = CH_3, R' = CH_2, R'' = H.

In the ethylperoxyl radical (R = C_2H_5), transfer of both α-hydrogen (R' = C_2H_5, R'' = H) (12) and methyl group (R' = CH_2, R'' = CH_3) (14) is possible. However, the latter process is energetically unfavorable (its barrier exceeds the activation barrier of the limiting initiation stage) and is therefore improbable (Tables 1, 9, 10).

$$C_2H_5OO^{\cdot} \longrightarrow CH_2O–{}^{\cdot}OCH_3, \quad (14)$$

$$CH_2O–{}^{\cdot}OCH_3 \longrightarrow CH_2O + CH_3O^{\cdot}. \quad (14')$$

A similar pattern is observed with molecular rearrangement of hydrocarbon hydroperoxides:

$$ROOH \longrightarrow R'O + R''O. \quad (15)$$

With methyl and ethyl hydroperoxides, in which the first stage is slow isomerization (transfer of α-hydrogen) and the second stage is fast elimination of water, reaction (15) can be presented as follows:

$$ROOH \longrightarrow R'O–OH_2, \quad (16)$$

$$R'O–OH_2 \longrightarrow R'O + H_2O, \quad (17)$$

Table 10. Geometries of the reaction center in process (14)

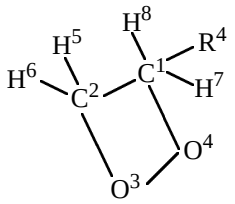

(14)

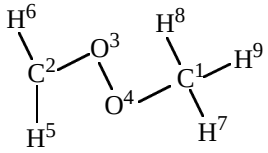

(14')

Parameter	Reactants		Transition state		Products	
	reaction (14)	reaction (14')	reaction (14)	reaction (14')	reaction (14)	reaction (14')
$C^1–C^2$	151.3	394.9	186.6	401.1	385.1	412.8
$C^2–O^3$	145.1	120.4	135.7	120.3	120.4	120.3
$O^3–O^4$	126.3	204.0	156.3	224.7	199.0	337.7
$O^4–C^1$	304.6	132.8	179.4	132.5	133.4	132.3
$\angle C^1C^2O^3$	112.1	26.76	104.39	31.25	26.09	53.87
$\angle C^2O^3O^4$	115.1	119.17	88.44	113.63	117.64	88.45
$\angle O^3O^4C^1$	51.1	119.03	99.41	114.59	114.69	86.62
$\angle C^1C^2O^3O^4$	80.72	0.18	0.0	–0.01	0.0	0.79
$\angle C^2O^3O^4C^1$	80.72	–179.72	0.0	179.99	180.0	178.01

Table 11. Main geometries of the reactants, products, and transition state of reactions (16) and (17)

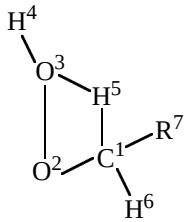

(16)

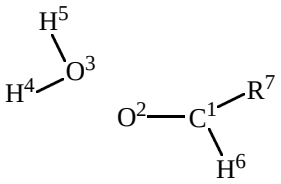

(17)

Parameter	Reactants				Transition state			
	reaction (16)		reaction (17)		reaction (16)		reaction (17)	
	R^7 = H	R^7 = CH_3	R^7 = H	R^7 = CH_3	R^7 = H	R^7 = CH_3	R^7 = H	R^7 = CH_3
$C^1–O^2$	138.8	139.7	120.3	121.1	128.2	129.2	120.4	121.0
$O^2–O^3$	152.5	152.6	208.3	210.8	177.8	176.7	217.4	214.0
$O^3–H^5$	339.2	253.6	95.2	95.2	150.6	150.8	95.2	95.1
$C^1–H^5$	109.5	110.7	331.8	332.3	136.1	137.9	328.9	330.7
$\angle C^1O^2O^3$	107.09	108.0	114.94	117.0	88.03	89.3	113.2	116.3
$\angle O^2O^3H^5$	30.10	54.8	102.45	98.3	75.23	75.20	95.1	95.5
$\angle H^5C^1O^2$	112.54	111.2	37.24	35.2	99.35	97.5	37.65	35.4
$\angle H^5C^1O^2O^3$	–62.18	51.0	22.52	23.7	0.0	4.0	22.5	–23.6

Table 11. (Contd.)

Parameter	Products			
	reaction (16)		reaction (17)	
	$R^7 = H$	$R^7 = CH_3$	$R^7 = H$	$R^7 = CH_3$
$C^1–O^2$	120.4	121.1	120.4	121.1
$O^2–O^3$	208.2	210.8	315.2	307.9
$O^3–H^5$	95.2	95.1	95.2	95.2
$C^1–H^5$	331.8	332.2	386.7	363.5
$\angle C^1O^2O^3$	114.96	116.9	179.75	124.3
$\angle O^2O^3H^5$	102.42	98.4	53.61	60.1
$\angle H^5C^1O^2$	37.2	35.2	11.42	35.0
$\angle H^5C^1O^2O^3$	–22.52	23.6	–91.33	20.8

where for methyl hydroperoxide R = CH_3, R' = CH_2; for ethyl hydroperoxide R = C_2H_5, R' = C_2H_4 (Table 11).

Similar to disproportionation of the ethylperoxyl radical, the molecular rearrangement of ethyl hydroperoxide can occur by two alternative mechanisms: transfer of α-hydrogen shown above (16) and transfer of the methyl group (18). However, in contrast to reaction (14), the methyl group is transferred in one stage (Table 12).

Table 12. Main geometries of the reactants, products, and transition state of elementary process (18)

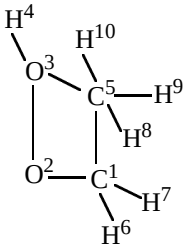

Parameter	Reactant	Transition state	Product
$C^1–O^2$	139.6	130.5	120.4
$O^2–O^3$	152.6	170.9	371.7
$O^3–C^5$	303.5	189.5	139.6
$C^1–C^5$	151.9	194.6	466.5
$\angle C^1O^2O^3$	108.0	87.9	61.5
$\angle O^2O^3C^5$	53.1	96.0	178.8
$\angle C^5C^1O^2$	113.9	109.5	105.0
$\angle C^5C^1O^2O^3$	–75.8	0.0	0.0

$$C_2H_5OOH \longrightarrow CH_2O + CH_3OH. \qquad (18)$$

Because the barrier to methyl transfer in the molecular rearrangement of ethyl hydroperoxide exceeds the

Table 13. Main geometries of the reactants, products, and transition state of reactions (20) and (21)

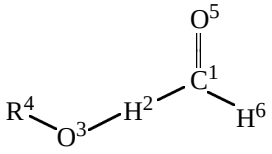

Parameter	Reactant		Transition state		Product	
	reaction (20)	reaction (21)	reaction (20)	reaction (21)	reaction (20)	reaction (21)
$C^1–H^2$	110.9	110.6	123.0	127.1	188.1	194.1
$H^2–O^3$	175.8	180.6	140.5	134.6	96.3	96.0
$O^3–R^4$	93.8	132.8	94.0	136.1	95.0	139.3
$C^1–O^5$	120.0	120.3	118.6	118.6	116.7	116.6
$C^1–H^6$	109.1	109.1	109.1	109.2	109.0	109.1
$\angle C^1H^2O^3$	169.27	179.98	179.8	175.3	178.95	170.79
$\angle H^2O^3R^4$	107.18	117.06	99.26	111.5	107.9	107.95
$\angle O^5C^2H^2$	121.28	121.58	121.3	121.3	120.23	120.42
$\angle H^6C^1H^2$	115.99	116.61	111.5	111.6	104.17	103.76
$\angle C^1H^2O^3R^4$	–0.36	173.12	1.20	–179.86	176.74	–179.57
$\angle O^5C^1H^2O^3$	0.34	–172.86	–1.61	180.0	179.63	–176.79
$\angle H^6C^1H^2O^3$	–179.66	7.14	178.44	0.0	3.16	–0.37

activation energy of the limiting stage (0) by almost 60 kJ mol^{-1} (Table 1), this reaction can also be excluded from consideration.

The reaction of aldehyde with oxyl radicals (19) was studied with two substituents:

$$RO^{\cdot} + CH_2O \longrightarrow ROH + H\text{–}C^{\cdot}\text{=}O, \quad (19)$$

$$HO^{\cdot} + CH_2O \longrightarrow H_2O + H\text{–}C^{\cdot}\text{=}O, \quad (20)$$

$$CH_3O^{\cdot} + CH_2O \longrightarrow CH_3OH + H\text{–}C^{\cdot}\text{=}O. \quad (21)$$

In both cases, a hydrogen-bonded prereaction complex is formed (Table 13), which somewhat decreases the sum of the energies of the reactants and increases the activation energy of the process.

Thus, the results obtained in this study allow us to discuss from a unified standpoint the minimal kinetic scheme of hydrocarbon oxidation with molecular oxygen. Certainly, additional studies are required to supplement data in Table 1 by ab initio estimates of the energy parameters of all the stages, to calculate the preexponential factors, and to consider in more detail the substituent effects.

Nevertheless, we can conclude that, on the whole, the results of our quantum-chemical study confirm the generally accepted mechanism of hydrocarbon oxidation with molecular oxygen and refine and supplement particular details of this mechanism. The results demonstrate the feasibility of quantum-chemical studies of the oxidation mechanism and can serve as a basis for further studies in this field.

REFERENCES

1. Potekhin, V.M., *Protsessy zhidkofaznogo avtookisleniya uglevodorodnogo syr'ya* (Liquid-Phase Auto oxidation of Hydrocarbon Raw Materials), Leningrad: Leningr. Tekhnol. Inst., 1983.
2. Semenov, N.N., *O nekotorykh problemakh kinetiki i reaktsionnoi sposobnosti* (Some Problems of Kinetics and Reactivity), Moscow: Akad. Nauk SSSR, 1954.
3. Semenov, N.N., *O nekotorykh problemakh khimicheskoi kinetiki i reaktsionnoi sposobnosti* (Some Problems of Chemical Kinetics and Reactivity), Moscow: Akad. Nauk SSSR, 1958.
4. Emanuel', N.M., Denisov, E.G., and Maizus, Z.K., *Tsepnye reaktsii okisleniya uglevodorodov v zhidkoi faze* (Chain Reactions of Liquid-Phase Oxidation of Hydrocarbons), Moscow: Nauka, 1965.
5. Tipper, S.F., *Okislenie uglevodorodov* (Oxidation of Hydrocarbons), Moscow: GINTI, 1960.
6. Emanuel', N.M., Zaikov, G.E., and Maizus, Z.K., *Rol' sredy v radikal'no-tsepnykh reaktsiyakh okisleniya organicheskikh soedinenii* (Role of the Medium in Radical-Chain Oxidation of Organic Compounds), Moscow: Mir, 1973.
7. Emanuel', N.M. and Gal, D., *Okislenie etilbenzola (model'naya reaktsiya)* (Oxidation of Ethylbenzene (Model Reaction), Moscow: Nauka, 1984.
8. Shtern, V.Ya., *Mekhanizm okisleniya uglevodorodov v gazovoi faze* (Mechanism of Gas-Phase Oxidation of Hydrocarbons), Moscow: Akad. Nauk SSSR, 1960.
9. Levitskii, A.A., Moshkina, R.I., and Polak, A.S., *Kinet. Katal.*, 1979, vol. 20, no. 5, pp. 1111–1117.
10. Sokolova, N.A., Markevich, A.A., and Nalbandyan, A.B., *Zh. Fiz. Khim.*, 1961, vol. 35, no. 4, pp. 850–857.
11. McDowell, C.A. and Thomas, J.H., *J. Chem. Phys.*, 1949, vol. 17, p. 588.
12. Denisov, E.T. and Kosarov, V.I., *Zh. Fiz. Khim.*, 1964, vol. 38, no. 12, pp. 2875–2881.
13. Denisov, E.T., *Kinet. Katal.*, 1994, vol. 35, no. 5, pp. 671–690.
14. Antonovskii, V.L., *Kinet. Katal.*, 1995, vol. 36, no. 3, pp. 370–378.
15. Denisova, T.G. and Denisov, E.T., *Zh. Fiz. Khim.*, 1991, vol. 65, no. 5, pp. 1208–1213.
16. Shen, D., Molse, A., and Pritchard, H.O., *J. Chem. Soc., Faraday Trans.*, 1995, vol. 91, no. 10, pp. 1425–1430.
17. Denisov, E.T., *Kinet. Katal.*, 1991, vol. 32, no. 2, pp. 461–465.
18. Baker, J., Stewart, J.P., Head-Gordon, M., Gonzalez, C., and Pople, J.A., *GAUSSIAN*, Pittsburgh, 1995.
19. Stewart, J.J.P., *J. Comput. Chem.*, 1989, vol. 10, no. 1, p. 221.
20. Lee, C., Yang, W., and Parr, R.G., *Phys. Rev. B*, 1988, vol. 37, pp. 785–789.
21. Becke, A.D., *J. Chem. Phys.*, 1993, vol. 98, no. 18, pp. 5648–5652.
22. Nikolaeva, E.V., Shamov, A.G., Khrapkovskii, G.M., and Kharlampidi, Kh.E., Abstracts of Papers, *VI Vserossiiskaya konferentsiya "Struktura i dinamika molekulyarnykh sistem"* (VI Russian Conf. "Structure and Dynamics of Molecular Systems"), Kazan, 1999, p. 149.
23. Nikolaeva, E.V., Shamov, A.G., Khrapkovskii, G.M., and Kharlampidi, Kh.E., Abstracts of Papers, *V Mezhdunarodnaya konferentsii po intensifikatsii neftekhimicheskikh protsessov "Neftekhimiya-99"* (V Int. Conf. on Intensification of Petrochemical Processes "Petrochemistry-99"), Nizhnekamsk, 1999, pp. 103–105.
24. Kondrat'ev, V.N., *Konstanty skorosti gazofaznykh reaktsii: Spravochnik* (Rate Constants of Gas-Phase Reactions: A Handbook), Moscow: Nauka, 1971.
25. Gurvich, L.V., Karachentsev, G.V., Kondrat'ev, V.N., Lebedev, Yu.A., Medvedev, V.A., Potapov, V.K., and Khodeev, Yu.S., *Energiya razryva khimicheskikh svyazei. Potentsialy ionizatsii i srodstvo k elektronu* (Dissociation Energies of Chemical Bonds. Ionization Potentials and Electron Affinity), Moscow: Nauka, 1974.